ELECTRIC FIELD EFFECTS ON THE NANOMETER-LEVEL SURFACE MODIFICATION OF Au(111) SURFACES

H. CABIBIL*, J. E. HOUSTON, T. M. MAYER and G. F. FRANKLIN
Sandia National Laboratories, Albuquerque NM
*University of Texas in Austin, Austin TX

ABSTRACT

We report observations of contrasting surface modification behavior of the of Au(111) in the presence of an electric field and field-emission currents using interfacial force microscopy (IFM) and scanning tunneling microscopy (STM). Our experiments consist of surface modification procedures which allow for large tip-sample gaps, in contrast to fast voltage pulses (applied at tunneling distances) employed by previous STM investigations. Dramatic surface distortions are observed when a 200 nm tip, biased at -100 V, is brought toward the Au surface to a field emission current level of 400 nA and then retracted. In other experiments, we raise the sample voltage to field-emission levels while maintaining a constant current. STM images, measured in a time-resolved manner after each such procedure, show that the presence of a higher electric field (~0.07 V/Å) results in step retraction and the disappearance of small islands on the Au(111) surface followed by the formation of vacancy islands in the area directly beneath the apex of the tip where the field is highest. We discuss the implications of these contrasting surface modification in terms of the various key parameters and in relation to previous studies using voltage pulses in the STM.

INTRODUCTION

The modification of Au surfaces to form nanostructures has been widely reported in the literature [1-6]. Generally, the creation of these structures (mounds and/or pits) involved the application of fast voltage pulses between tip and sample at tunneling distances in the scanning tunneling microscope (STM). Mechanisms proposed include positive and/or negative field evaporation between the Au sample and Au tip [1-5] and electroetching [6]. Other STM investigations [7-8], however, presented compelling evidence that the mound/pit formation is due to actual mechanical contact between tip and sample as a result of tip/sample deformation during pulsing. We have therefore carried out experiments in a more controllable manner by allowing for larger tip-sample separations which avoids tip/sample contact. Our results, which were obtained from a UHV-IFM/STM system, varies from mound formation, observed at relatively high field emission currents to step retraction and vacancy island formation observed at much lower field emission currents. These results definitely rule out processes such as field evaporation and mechanical contact between tip and sample, but question about the details of the interactions is still unclear.

EXPERIMENT

The experiments were carried out in an ultra-high-vacuum (UHV) chamber with capabilities for interfacial force microscopy (IFM), scanning tunneling microscopy (STM), ion sputter cleaning and Auger Electron Spectroscopy. IFM is a scanning force microscopy similar to the atomic force microscope but is distinguished by its use of a stable, self-balancing force sensor [9]. The tip used is W, formed by electrochemical etching of a 100 micron wire. The sample used is a Au(111) crystal. Sample treatment and vacuum conditions differ for each surface modification procedure employed. These procedures and experimental conditions are outlined below.

Current/Force Profile Measurements

To circumvent the problem presented by operating at tunneling distances, we carry out our surface modification by translating the W tip from a distance of approximately 1000 Å, towards the Au(111) surface at constant potential while monitoring the field-emission current. We allow the tip to approach until a preset turnaround current is reached. A current profile measurement therefore consists of plots of field emission current vs. tip-sample separation. (Similarly, IFM

DISCLAIMER

DISCLAIMER

Portions of this document may be illegible electronic image products. Images are produced from the best available original document.

force profiles consist of plots of electrostatic force between tip and sample vs. tip-sample separation). Both current and force profile measurements were carried out simultaneously using the IFM. The quantitative separation scale was obtained by correlating the initial-point separation with the tip-sample gap established upon translating the tip towards the sample until contact is made. The Au(111) crystal is Ar ion sputter-cleaned at room temperature but not annealed. Therefore some surface roughness was to be expected. The chamber base pressure is ~ 3×10^{-10} Torr.

V-Z Measurements

These measurements were carried out with the system in the STM mode. The V-Z surface modification procedure consists of slowly increasing the bias voltage while the feedback loop is operational causing the tip to retract in order to maintain the setpoint current. The Au(111) crystal was Ar ion sputtered and annealed ex-situ. The crystal is therefore exposed to air for a few hours before insertion to the STM chamber for image and manual V-Z measurements. The chamber base pressure is ~ 3×10^{-10} Torr.

RESULTS AND DISCUSSION

Current/Force Profile Measurements

The variation of the field-emission current with respect to relative tip-sample separation for a tip bias of -100 V and a turn-around current of 100 nA is shown in Fig. 1a. This plot shows that the current follows an exponential behavior with no hysteresis between approach and withdrawal. In Fig. 1b, we show the manner in which the interfacial electrostatic force between tip and sample varies corresponding to the current behavior of Fig. 1a. Again, the force follows the expected reciprocal relationship with separation and shows no hysteresis between approach and withdrawal. However, if this same type of data is taken at a turn-around current value of 400 na, from the same starting separation, we obtain the behavior shown in Fig. 2a. Up to a tip/sample separation of about 460 Å, the current behaves in the same manner as seen in Fig. 1a. However, for smaller separations, the current rises more rapidly than exponential, accelerating until the tip begins its retraction at about 400 Å. At this point, the current remains essentially constant for about the first 50 Å of withdrawal and then gradually settles into an exponential decrease. The approach and withdrawal curves of Fig. 2a appear shifted by about 140 Å and the withdrawal data has a slightly higher slope on the semilog plot. In contrast, Fig. 2b shows the force curve corresponding to the current behavior shown in Fig. 2a. As for the current, the force follows the expected separation dependence down to values of approximately 460 Å, at which point it begins to rise. However, unlike the current, after turn-around the force settles back to follow the 1/d path of the approach curve (the 1/d relationship is shown as the solid curve in Fig. 2b). This reflects the long-range origins of the force. After back off about 250 Å, the 140 Å modification does not appreciably affect the force relative to the original flat surface.

It is clear from the plots in Fig. 1 and 2 that the surface has distorted as a result of the approach to the maximum of 400 nA current. The distortion is better depicted in Fig. 3a, which shows the level of surface deformation as a function of time. This plot is obtained by taking the differences of the approach and withdrawal data and the expected "no distortion" exponential behavior. The time axis is derived by dividing the displacement of Fig. 1a by the 25 Å/sec translation rate. We see in Fig. 3a that the surface comes out to meet the tip by about 140 Å over a period of several seconds. The speed of this surface distortion can be found by taking the derivative of the data of Fig. 3a and this result is shown in Fig. 3b. Here we see that the surface velocity rapidly increases to a maximum value of approximately 30 Å/sec and remains near this value for about one second. The surface distortion takes place in only a few seconds.

There are several possible explanations for the surface distortion observed here involving the electric field and the field-emission current. The electric field can facilitate surface modification in several ways: field evaporation, stress-mediated mechanical deformation, field and field-gradient induced diffusion of atoms and surface electromigration. Negative field evaporation (from tip to sample) can be easily excluded as the cause of the distortion because the field strength achieved at the turn-around point, calculated as voltage/separation, is only 0.22 V/Å. This value is almost an

order of magnitude lower than the required field value for field evaporation based on model calculations which corrected for the close proximity between the tip and surface [10]. Mechanical deformation due to the surface electrostatic stress (stress varies as E^2) is also a possible player in the surface distortion. We have calculated the elastic deformation using our experimental conditions and found an elastic distortion value of only 1 Å. Additionally, calculations for the threshold electrostatic surface stress for plastic deformation results in a value of only 43 Mpa, a value well below the yield stress of about 1 Gpa [11]. It seems certain that the surface motion in Fig. 3a is not affected by either elastic or plastic deformation under our experimental conditions. Finally, there is the issue of a field or field-gradient induced surface diffusion. The electric field gradient induces diffusion which arises from the localization of the field by the STM tip. The gradient sweeps metal atoms toward the maximum-field value directly beneath the tip and, if the gradient is strong enough, cause an accumulation of atoms in this region. In terms of field effects, field-gradient-induced surface diffusion is a possible key player in the surface distortion observed from our current profile data, where the field gradients are large and the high currents encourage enhanced diffusion [12]. The high field emission current can also facilitate distortion by either localized surface heating or electromigration (or both).

As a clue to the possible mechanism, we have assumed that the process is activated and that the effect is proportional to the power delivered, which is in turn proportional to the current squared. Thus, the rate of surface distortion would be modeled by an exponential of a negative constant divided by the current squared. Such a model, parameterized to produce the best agreement, is shown in Fig. 3c and shows a remarkably good agreement. It is, in fact, the only model that we could find that adequately modeled the vary rapid rise and fall of the surface distortion shown in Fig. 3b. This crude model suggests that the current is a key feature and would tend to support either a local temperature rise or possibly electromigration.

V-Z Measurements

In contrast to the implications of the results presented above, a different phenomenon occurs when a V-Z cycle is used as the procedure for surface modification. Fig. 4 illustrates the behavior during a series of sequential V-Z cycles followed by 200 nm x 200 nm STM images of the surface. Each V-Z cycle requires about one min. The initial surface (Fig. 4a) shows a major pinning site surrounded by a distribution closely spaced individual steps and a large terrace populated by small islands. These islands were found to be present on the Au(111) surface after an ex-situ sputter-anneal treatment. Fig. 4b shows the same surface after three V-Z cycles from an initial sample tunneling bias of +0.10 V to +75 V at a constant current of 0.5 nA. One can see that the islands have disappeared and that a one monolayer deep vacancy island has formed (Intermediate images show that the islands rapidly disappear with V-Z cycles and that the vacancy island only slowly grows after initial nucleation). However, Figures 4c through 4f indicate that once the bridge between the neighboring step edge and the vacancy island is breached, the vacancy island grows rapidly. In addition, once the vacancy island has reached a relatively large size, a second island begins to form on the floor of the original island. Notice also that during the course of these experiments the terraces leading from the pinning site have all gotten wider indicating a general smoothening of the local surface.

These modifications were found to be independent of field direction and, therefore, electromigration can be ruled out as a possible mechanism. We can also exclude a current-induced diffusion due to localized heating, since the currents used are very small. This leaves us with field effects as the probable cause of the observed modifications. As mentioned earlier, the presence of large field gradients can lead to atom accumulation under the tip due to metal-atom polarization effects. Our model calculations, using parameters from our experimental conditions and the results just described, indicate that the effect of the field gradient on the surface potential is small. This results from the rather large tip radius and the large tip/sample separation at the V-Z voltages. On the contrary, the effect clearly involves a field-induced weakening of the thermal barrier to island edge evaporation onto the terrace surface followed by rapid diffusion away from the high field region. Larger-scale images such as in Fig. 4 indicated that the smoothening effect only takes place over an area with about a 250 nm diameter. The slow initial growth of the vacancy island indicates that the process of an atom mounting the up-step edge surrounding the island is small compared to the probability of island-edge desorption. However, once the bridge to the

neighboring down-step edge is breached, the mobile atoms in the vacancy island pour out and diffuse away from the high-field region resulting in rapid vacancy island growth.

CONCLUSIONS

We have presented the results of two contrasting schemes for the controlled modification of the Au(111) surface indicating the formation of either a mound or a vacancy island depending on the surface modification procedure employed. These effects cannot be attributed to either field evaporation or mechanical tip/sample contact. We believe that the mound formation indicated in our current-profile measurements is driven by the high and very localized currents encountered in this procedure, which suggests either a temperature enhanced diffusion or possibly an electro-migration-driven process. While the results from the current-profile measurements indicate that atoms are being drawn towards the area of the highest field, the V-Z experiments show atoms leaving the area of the highest field under only the influence of a somewhat lower field and greatly reduced field gradient. The details of the delicate balance between opposing forces that controls these two processes remains illusive. However, future work involving an extended exploration of the parameter space and better prepared surfaces should allow us to elucidate the detailed physics behind these interesting field-induced processes for surface-modification and yield more controllable methods for producing tailored nanostructures.

ACKNOWLEDGMENTS

Support for this work by the U.S. Department of Energy is acknowledged. Special thanks to R. Q. Hwang of Sandia National Labs - Livermore CA, J. M. White of the University of Texas - Austin, X. Y. Zhu and H. Wang of the University of Minnesota.

REFERENCES

1. H.J. Mamin, S. Chiang, H. Birk, P.H. Guethner and D. Rugar, J. Vac. Sci. Technol. B **9**(2), 1398 (1991).
2. H. J. Mamin, S. Chiang, P.H. Guethner and D. Rugar, Phys. Rev. Lett. **65**(19), 2418 (1990).
3. Ch. Mascher and B. Damaschke, J. Appl. Phys. **75**(10), 5438 (1994).
4. S.E. McBride and G.C. Wetsel, Jr., Appl. Phys. Lett. **59**(23), 3056 (1991).
5. Y.Z. Li, L. Vasquez, R. Piner, R.P. Andres, and R. Reifenberger, Appl. Phys. Lett. **54**(15), 1424 (1989).
6. C.S. Chang, W.B. Su, and Tien T. Tsong, Phys. Rev. Lett. **72**(4), 574 (1994).
7. J.I. Pascual, J. Mendez, J. Gomez-Herrero, A.M. Baro, and N. Garcia, Phys. Rev. Lett. **71**(12), 1852 (1993).
8. R.Taylor, R.S. Williams, V.L. Chi, G. Bishop, J. Fletcher, W. Robinett, S. Washburn, Surf. Sci. Lett. **306**, L534 (1994).
9. S.A. Joyce and J.E. Houston, Rev. Sci. Instrum., **62**(3), 710(1991).
10. T.T. Tsong, Phys. Rev. B **44**(24), 13 703 (1991).
11. T. A. Michalske and J. E. Houston, Acta. Metall. **46**, 391 (1998)].
12. T. M. Mayer, H. Cabibil and J. E. Houston (To be Published).

Figure 1. (a) Field-emission current vs. tip/sample separation with approach and withdrawal at 25 Å/sec to a maximum current of 100 nA. (b) interfacial force over the same

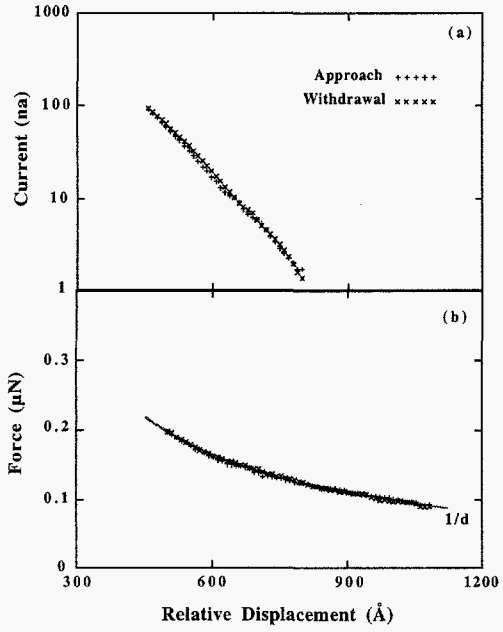

Figure 2. The same procedure as in Fig. 1 but to a maximum current of 400 nA.

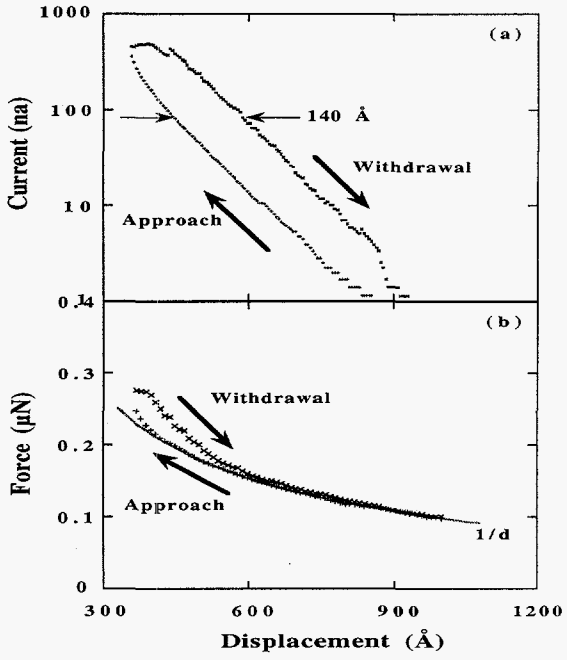

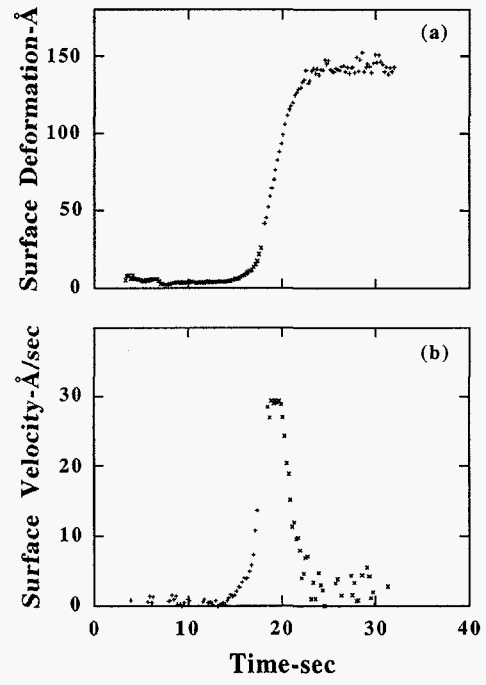

Figure 3. (a) surface distortion vs. the experimental time for the data of Fig. 2a . (b) the rate of surface distortion (c) a surface-rate model plotting exp ($-5x10^5/I^2$) vs. time.

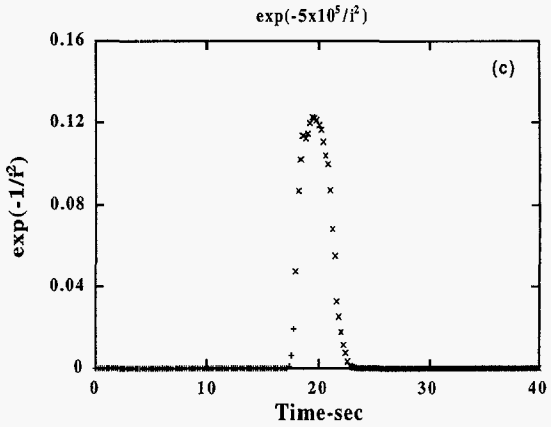

Figure 4. STM images of a sequency of V-Z surface-modification cycles: (a) shows the original surface with a pinning site in the upper left hand corner surrounded by a steep step distribution and a large terrace covered by small islands, (b) the surface after 3 V-Z cycles to +75 V at 0.5 nA (each cycle takes about 1 min.), (c)-(f) surface appearance after sequential V-Z cycles. Time duration noted in each frame is cumulative.

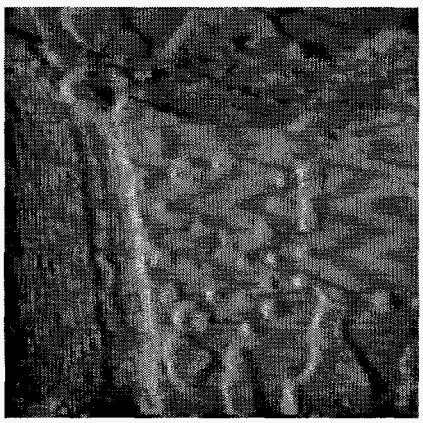

(a) t = 0

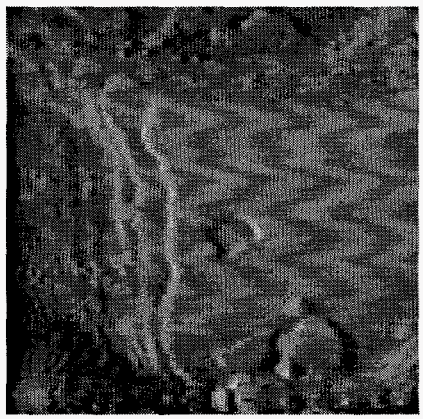

(b) t = 3 min

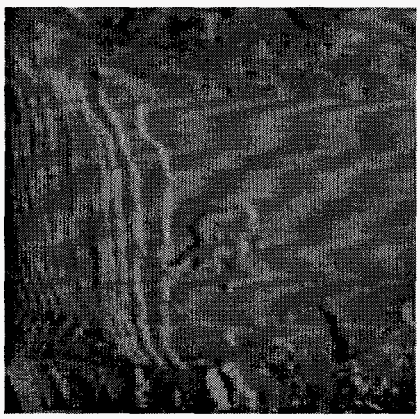

(c) t = 5 min

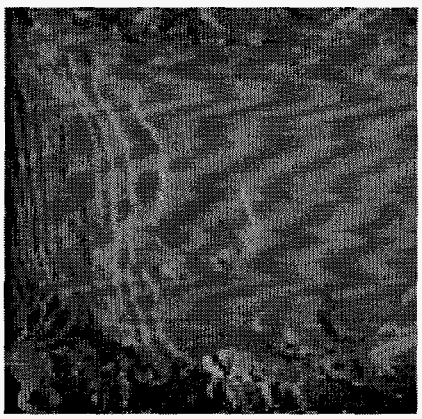

(d) t = 7 min

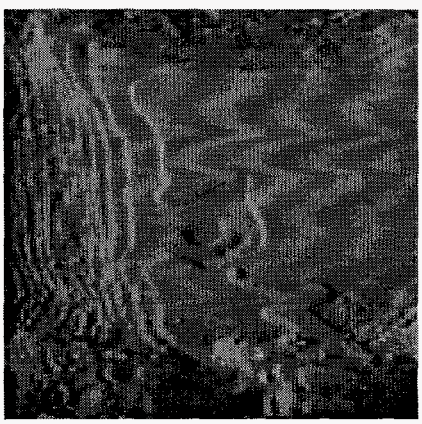

(e) t = 9 min

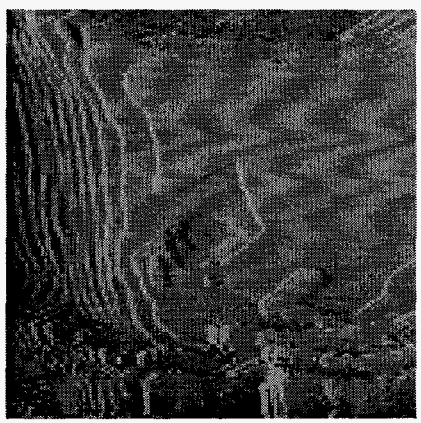

(f) t = 11 min